Neural Networks and Support Vector Machine Algorithms for Automatic Cloud Classification of Whole-Sky Ground-Based Images

Alireza Taravat, Fabio Del Frate, Cristina Cornaro, and Stefania Vergari

***Abstract*—Clouds are one of the most important meteorological phenomena affecting the Earth radiation balance. The increasing development of whole-sky images enables temporal and spatial high-resolution sky observations and provides the possibility to understand and quantify cloud effects more accurately. In this letter, an attempt has been made to examine the machine learning [multilayer perceptron (MLP) neural networks and support vector machine (SVM)] capabilities for automatic cloud detection in whole-sky images. The approaches have been tested on a significant number of whole-sky images (containing a variety of cloud overages in different seasons and at different daytimes) from Vigna di Valle and Tor Vergata test sites, located near Rome. The pixel values of red, green, and blue bands of the images have been used as inputs of the mentioned models, while the outputs provided classified pixels in terms of cloud coverage or others (cloud-free pixels and sun). For the test data set, the overall accuracies of 95.07%, with a standard deviation of 3.37, and 93.66%, with a standard deviation of 4.45, have been obtained from MLP neural networks and SVM models, respectively. Although the two approaches generally generate similar accuracies, the MLP neural networks gave a better performance in some specific cases where the SVM generates poor accuracy.**

***Index Terms*—Automatic classification, cloud classification, neural networks, support vector machine, whole-sky images.**

I. Introduction

CLOUD coverage or cloud fraction measurements are generally used for flight planning and aviation. On the other hand, they have a strong impact on the radiation budget and on the climate change and variability [1]. More recently, with the growing interest on renewable energy sources (especially solar energy), information about cloud coverage earned additional importance for the electricity production forecast from photovoltaic and solar power systems [2].

The feedbacks of low clouds (a negative feedback) and high thin clouds (a positive feedback) on the radiation budget are well known. Reflection and absorption by cloud particles depend on the volume, shape, and thickness of the clouds [3]. In this context, ground-based imaging devices are commonly used to support satellite studies. There are several reasons for using ground-based sensors for cloud recognition: 1) localized (immediately overhead) cloud presence in a given area cannot be determined using satellite images with high accuracy, and 2) ground-based imaging sensors are cheaper in comparison with spaceborne platform images [4].

In the related literature, there are many papers which demonstrate the increased number of ground-based instruments for whole-sky image acquisitions [5]. Thus, suitable and adequate image processing procedures are necessary to fully exploit the huge amount of data available.

Bush *et al.* provided a classification method based on the binary decision trees in order to classify the ground-based images into five different sky conditions [6]. Singh and Glennen utilized cooccurrence and autocorrelation matrix for ground-based cloud recognition [4]. Calbo and Sabburg used Fourier transformation to classify eight predefined sky conditions [7]. Liu *et al.* extracted some cloud structure features from infrared images [8]. Heinle *et al.* proposed an approach based on textural features such as energy and entropy as an automated classification algorithm for classifying seven different sky conditions [3].

Machine learning approaches such as multilayer perceptron (MLP) neural networks and support vector machines (SVMs) have already been demonstrated to provide excellent performance in the classification of remotely sensed images. Both techniques are effective as they build input-output relationships directly from the data without the need of *a priori* assumptions or specific preprocessing procedures. Another advantage is that, once the training phase is over, the classification is basically obtained in real time with a strong reduction of the computational burden.

A combination of neural networks with sky image data has been recently proposed for direct normal irradiance forecasting models [9]. However, to our knowledge, a detailed analysis of different machine learning models for automatic classification of whole-sky images has not been presented so far in the literature, whereas machine learning models can be very competitive in terms of accuracy and speed for image classification. Starting from these motivations, the purpose of the present paper is to demonstrate the potential of the machine learning approach for a fast, robust, accurate, and automated whole-sky image classification approach. The rest of this letter is organized in four sections. In the following section, the cloud camera

Manuscript received June 3, 2014; revised August 14, 2014; accepted September 6, 2014.

A. Taravat and F. Del Frate are with the Department of Civil Engineering and Computer Science, University of Rome "Tor Vergata," 00133 Rome, Italy (e-mail: art23130@gmail.com).

C. Cornaro is with the Department of Enterprise Engineering, University of Rome "Tor Vergata," 00133 Rome, Italy.

S. Vergari is with the Center of Meteorological Experimentation, Italian Air Force, 00062 Rome, Italy.

Color versions of one or more of the figures in this paper are available online at http://ieeexplore.ieee.org.

Digital Object Identifier 10.1109/LGRS.2014.2356616

Fig. 1. The SRF-01 Cloud Cam at the centre of meteorological experimentation (Re.S.M.A.) of Vigna di Valle.

and the associated image data are introduced. Section III contains a description of the methodology behind the proposed approach. The results, discussion, and conclusion follow in Sections IV and V.

II. Camera

Only a few research institutions in several countries have developed noncommercial sky cameras for their own requirements [3], [5], [10]. The automatic sky imaging system which has been used for this experiment is the SRF-01 Cloud Cam that is a commercial sky camera produced by EKO (Fig. 1). The SRF-01 Cloud Cams have been installed at the Centre of Meteorological Experimentation (Re.S.M.A.) of Vigna di Valle ($42°06'$ N, $12°12'$ E; 266 m a.s.l.) and at the Solar Energy Test and Research Laboratory (SETR Lab) of Tor Vergata University ($41°51'$ N, $12°35'$ E), South-East of Rome [11].

The main device consists of a Canon Power Shot A60 digital camera in a weatherproof housing, with a maximum resolution of 1600 $\times$ 1200 pixels in 30-b color JPEG format. Additional optics extends the field of view to 180°, providing the possibility to make color pictures of the sky. The images are rectangular, but the whole sky mapped is circular. The center of the circle is the zenith, and the horizon is along the border (more details in Kalisch *et al.*) [3], [10].

The Cloud Camera has been set to acquire two photographs every 10 min. The first one is well exposed (aperture $= 1/500$ and shutter $= 8.0$), and the second one is lightly under exposed (aperture $= 1/1000$ and shutter $= 8.0$), which are the optimum cloud camera settings achieved by [11]. The algorithm for cloud detection offered by EKO Co. needs both well-exposed and under-exposed images for sun identification, but in this study, only the acquisitions from the first exposure mode have been used for the machine learning algorithms. The PC clock has been set on UTC, and the daily time interval of image acquisition was from 5 A.M. to 9 P.M. in order to consider the period from sunrise to sunset.

III. Methods

The considered data set contains an overall number of 250 images, 200 from the Vigna di Valle ($42°06'$ N, $12°12'$ E) test site and 50 from the Tor Vergata University ($41°51'$ N, $12°35'$ E) test site. These 250 images contain all different types of clouds under a variety of sky conditions at different selected day times and seasons. The data set has been categorized into four groups (Table I) according to the International Cloud Classification System published in WMO (1987). In order to avoid systematic misclassifications, we have merged some of the classes (altostratus and stratus, cirrocumulus, and altocumulus). Additionally, the genera cirrus and cirrostratus have been merged due to the difficulty in detecting very thin clouds (such as some kinds of cirrostratus). Despite these generalizations, the resulting classes represent a suitable partitioning of possible sky conditions which are especially useful for radiation studies.

As a preprocessing task, the interesting part (which is circular in shape) of each image in the data set has been extracted, and then, disruptive factors like camera antenna or trees have been eliminated from the subset images. The preprocessing phase makes classification and image interpretation more expedient and accurate.

After the preprocessing phase, all of the images have been classified by MLP neural networks and SVM classifiers. Then, the results have been analyzed and compared with each other and with the results of the multiband thresholding algorithm (which is the combined result of AND operations for thresholded red, green, and blue bands of the images), which is a very popular method in this field offered by EKO Co., and with the results of the k-nearest neighbor classifier presented by Heinle *et al.* [3], which is the latest paper published in the related literature about automatic cloud classification of whole-sky images.

TABLE I
Cloud-Type Categories

Group	Cloud Categories
1	Clear Sky (No cloud or cloudiness less than 5%)
2	Stratus, altostratus, Nimbostratus (Low or mid-level layer of dark, thick clouds, uniform, usually overcast, gray)
3	Stratocumulus, Cumulus (Low or mid-level, puffy or lumpy layer of clouds, white or gray)
4	Cirrus, Cirrostratus, Altocumulus, Cirrocumulus (High patched of small cloudlets, thin clouds, mosaic, wisplike, white)

TABLE II
Min, Max, and Average Values (Computed Over the Number of the Images Considered in Each Group) of the Accuracies for Different Types of Clouds Classified by MLP and SVM (in Percent)

Group	Model	Min	Max	Mean	St.Dev
1	MLP	97.00	99.50	98.65	0.61
	SVM	97.94	99.10	97.92	0.80
2	MLP	95.00	98.18	96.62	0.71
	SVM	90.20	97.20	95.74	1.92
3	MLP	85.00	97.00	93.36	2.93
	SVM	84.70	96.30	93.02	3.31
4	MLP	84.88	95.00	91.63	2.40
	SVM	80.92	92.00	88.03	3.03

TABLE III
AVERAGE VALUES OF COMMISSION AND OMISSION ERRORS (IN PERCENT) ACHIEVED BY MLP AND SVM FOR DIFFERENT GROUPS OF DATA

Group	Method	MinOm	MaxOm	MeanOm	St.DevOm	MinCm	MaxCm	MeanCm	St.DevCm
1	MLP	0.50	3.00	1.33	0.62	1.00	10.00	5.14	2.32
	SVM	0.9	3.00	2.08	0.82	3.00	8.10	5.25	1.47
2	MLP	1.82	5.00	3.37	0.73	1.20	8.80	4.35	2.48
	SVM	2.80	9.8	4.25	1.93	3.1	9.2	4.78	2.10
3	MLP	3.00	15.00	6.64	2.93	2.50	13.60	8.91	2.42
	SVM	3.70	15.30	6.97	3.31	4.50	12.60	8.93	2.13
4	MLP	5.00	15.12	8.37	2.41	4.20	14.20	10.12	3.04
	SVM	8.00	19.08	12.04	3.02	6.2	14.6	10.53	2.42

MLPs are a very powerful neural network model for pixel-level classification [12], [13], which is trained by the error back-propagation algorithm (the most commonly used model from feedforward family). In the MLP model, the number of units in the hidden layer and the training phase settings (the number of training cycles and the pixel selection for training/testing the model) represent the fundamental tasks. Normalization, which is a preliminary phase of neural network classifications, is performed by linear transformation from the image interval [0–255] to the neural network interval $[1, 1]$ (the normalization phase ensures that the distance measures respond with equal weight for each input) [14].

A radial basis function kernel, a very powerful kernel for pixel-level classification [15], has been selected as the primary SVM kernel function. In SVM (with radial basis function as the kernel), the setting of C and γ represents the fundamental task in the phase of model designing.

Adjustment of the mentioned parameters (for MLPs and SVM) affects the capability and sensitivity of the models to fit the dynamic ranges of the pixel values in the images. The IDL programming software for the preprocessing phase and the neural network simulator (SNNS) developed at the University of Stuttgart, Stuttgart, Germany, have been used in implementing the classification algorithms. Also, the SVM software (SVM-Light package; URL: http://svmlight.joachims.org) has been used for SVM processing.

IV. RESULTS AND DISCUSSION

In the MLP classifier, 5423 pixels (extracted from 15 images) have been used for training/testing the net. These 15 images contain all different types of clouds under a variety of sky conditions at different selected times during the day. The training sets contain 60% of the data, and the test sets contain the remaining 40% which do not belong to the training sets. Pixel selection for the training/test set has been performed randomly and repeated four times.

Several attempts have been made to properly select the number of units to be considered in the hidden layers of the MLP. Architecture 3-7-2 has been finally chosen for its good performance in terms of classification accuracy, root-mean-square error (rmse), and training time. Here, 10 000 training cycles were sufficient to train the network. The inputs of the net consist of red, green, and blue bands, and the output provides the pixel classification in terms of cloudy pixel or others (cloud-free pixels or sun). One MLP has been used in classifying all of the images.

In the SVM classifier, the images have been rescaled between (0.0–1.0) for training the model. A range of values was tested for the two SVM parameters C (1–50) and γ (0.1–10). A grid search method has been used to examine the various combinations of C and γ, and the best combination has been finally chosen based on the model performance in terms of classification accuracy and rmse [16].

The training/test sets are exactly the same as those which have been used for the MLP classifier. Pixel selection for the training/test set has been again done randomly and repeated four times. Random pixel selection allows us to examine the robustness of the classification algorithms with respect to the variability of the training data set [16]. For the validation phase and accuracy assessment, from each image in the data set, 250 pixels have been selected randomly and then labeled by visual interpretation.

The accuracy of the whole test data set classified by MLP is 95.07%, with a standard deviation of 3.37, while the accuracy of the SVM classifier is 93.66%, with a standard deviation of 4.45. The average accuracy achieved by the EKO classification technique is 50.90%, with a standard deviation of 11.25%. Visual inspection shows that the machine learning approaches (MLP and SVM) achieve much better detection results under a variety of conditions in comparison with the results of the multiband thresholding algorithm. In Heinle's work [3], the average accuracy which has been obtained is about 88%. Moreover, the k-nearest neighbor classifier presented by Heinle *et al.* is characterized by slow runtime performance and large memory requirements [3], whereas the classification by the artificial neural network approach with a 1000×1000 image can be completed in about a few seconds on a personal computer with an Intel Pentium dual-core, a speed of 2.2 GHz, and a RAM memory of 2.00 GB, which is much faster than some existing methods in the literature. This might have a significant impact on the reduction of the computational burden when large data sets need to be processed.

The results of the accuracy assessment applied to different types of clouds are displayed in Tables II and III.

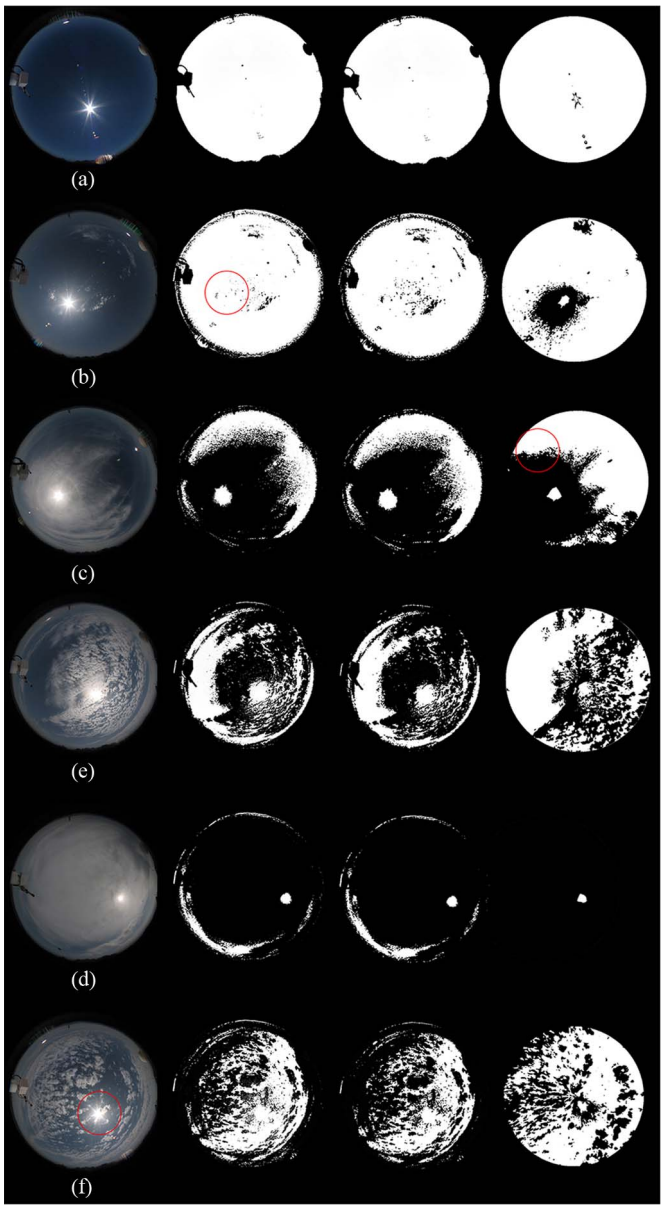

Fig. 2. Classification results of six typical examples. (a) and (b) Clear-sky example (no clouds and cloudiness below 5%). (c) and (d) Example of the detection of low or midlevel layer of uniform clouds and dark thick clouds. (e) Example of the detection of low puffy clouds with clearly defined edges and high thin clouds, wisplike. (f) Example of the detection of high patched clouds of small cloudlets, mosaiclike. (First column) Original images. (Second and third columns) Results of the MLP and SVM classifiers. (Last column) Results of the classification offered by EKO Co.

The MLP classifier generates a satisfactory accuracy on the clear-sky, stratus-altostratus-nimbostratus, and stratocumulus-cumulus groups. The average accuracy of the clear-sky class is 98.65%, with a standard deviation of 0.61. The average commission (percentage of extra pixels in the class) and omission (percentage of pixels left out of the class) errors of the clear-sky class are 5.14% and 1.33%, respectively. In the case of the stratus-altostratus-nimbostratus group, the average accuracies of 96.62% (standard deviation of 0.71%) with 4.35% and 3.37% commission and omission errors are obtained by the MLP classifier. The accuracy of the same groups classified by SVM are 97.92%, with a standard deviation of 0.80% (5.25% and 2.08% commission and omission error averages), and 95.74%, with a standard deviation of 1.92% (4.78% and 4.25% commission and omission error averages).

A significant improvement of 3.60% in accuracy (with a difference of 0.63% in standard deviation) has been obtained on the cirrus-cirrostratus-altocumulus-cirrocumulus group segmented by MLP with respect to the same data set segmented by SVM (the average accuracy is 88.03%, with a standard deviation of 3.03%).

It is necessary to identify the situations where the proposed approaches generated poor accuracy and see why the models failed to work correctly in those cases. The worst accuracy generated by the MLP classifier is 84.88% with 14.20% commission error, which is obtained for the cirrus-cirrostratus-altocumulus-cirrocumulus group. This accuracy is 3.96% higher than the worst accuracy obtained by the SVM classifier which is for cirrus-cirrostratus-altocumulus-cirrocumulus group (80.92% with 14.60% commission error).

This low performance is caused by the thin and transparent parts of cirrus clouds which cannot be detected by both algorithms (these parts have been classified as clear sky). Moreover, the so-called "whitening effect" provides a misclassification of cloud-free pixels (which are brighter due to forward scattering by aerosols and haze) near the solar disk, and therefore, such pixels are classified as thin clouds by the algorithms (see also [3] and [17]). Fig. 2(b), (c), and (f) illustrates the typical examples where the models generate less accuracy.

V. Conclusion

In the present study, the capabilities of machine learning algorithms as automated methods for cloud segmentation in whole-sky images have been demonstrated. Two classification algorithms (MLP neural networks and SVM) have been compared using a data set containing 250 images from two different test sites. The same parameters were used for all of the test images.

The obtained accuracies showed that the machine learning approaches (MLP and SVM) achieve better detection results under a variety of conditions with respect to the results of the thresholding algorithm, which is a popular model for whole-sky image classification. The machine learning models generate lower accuracies for the cirrus-cirrostratus-altocumulus-cirrocumulus group (caused by cirrus clouds), and in some other cases, the accuracy is decreased because of the whitening effect near the solar disk. The results show that the MLP classifier as an automated algorithm for cloud classification works better in the situations where SVM generates poor accuracy.

Acknowledgment

The authors would like to thank the associate editor and the anonymous reviewers for their constructive comments, Colonel F. Foti and Captain E. Vuerich from the Centre of Meteorological Experimentation of the Italian Air Force for hosting the cloud camera in their field at Vigna di Valle, the Misure company for kindly providing the Cloud Camera, and Dr. T. Vitti from Tecnoel Company for the installation and assistance.

REFERENCES

[1] Z. Chen, D. Zen, Q. Zhang, and D. Ginthner, "Sky model study using fuzzy mathematics," *J. Illuminating Eng. Soc.*, vol. 23, no. 1, pp. 52–58, 1994.

[2] M. Martinez-Chico, F. J. Bathes, and J. L. Bosch, "Cloud classification in a Mediterranean location using radiation data and sky images," *Energy*, vol. 36, no. 7, pp. 4055–4062, Jul. 2011.

[3] A. Heinle, A. Macke, and A. Srivastav, "Automatic cloud classification of whole sky images," *Atmos. Meas. Technol.*, vol. 3, no. 3, pp. 557–567, Jan. 2010.

[4] M. Singh and M. Glennen, "Automated ground-based cloud recognition," *Pattern Anal. Appl.*, vol. 8, no. 3, pp. 258–271, Nov. 2005.

[5] G. Pfister *et al.*, "Cloud coverage based on all-sky imaging and its impact on surface solar irradiance," *J. Appl. Meteorol.*, vol. 42, no. 10, pp. 1421–1434, Oct. 2003.

[6] K. A. Bush, C. H. Sun, and L. R. Thorne, "Cloud classification using whole-sky imager data," in *Proc. 9th Symp. Meteorol. Observ. Instrumentation*, 1995, pp. 353–358.

[7] J. Calbo and J. Sabburg, "Feature extraction from whole-sky ground-based images for cloud-type recognition," *J. Atmos. Ocean. Technol.*, pp. 3–14, 2008.

[8] L. Liu, X. J. Sun, F. Chen, S. J. Zhao, and T. C. Gao, "Cloud classification based on structure features of infrared images," *J. Atmos. Ocean. Technol.*, vol. 28, no. 3, pp. 410–417, Mar. 2011.

[9] Y. H. Chu, H. T. C. Pedro, and C. F. M. Coimbra, "Hybrid intra-hour DNI forecasts with sky image processing enhanced by stochastic learning," *Solar Energy*, vol. 98, pp. 592–603, Dec. 2013.

[10] J. Kalisch and A. Macke, "Estimation of the total cloud cover with high temporal resolution and parametrization of short-term fluctuations of sea surface insolation," *Meteorologische Zeitschrift*, vol. 17, no. 5, pp. 603–611, Oct. 2008.

[11] C. Cornaro, S. Vergari, F. Foti, and F. Del Frate, "Project CL.E.A.R. Cloudiness Experiment For Automatic Recognition," in *Proc. TECO WMO Tech. Conf. Meteorol. Environ. Instruments Methods Observ.*, Brussels, Belgium, Oct. 16–18, 2012, pp. 1–9.

[12] J. F. Mas and J. J. Flores, "The application of artificial neural networks to the analysis of remotely sensed data," *Int. J. Remote Sens.*, vol. 29, no. 3, pp. 617–663, Feb. 1, 2008.

[13] A. Taravat and F. Del Frate, "Development of band ratioing algorithms and neural networks to detection of oil spills using Landsat ETM plus data," *EURASIP J. Adv. Signal Process.*, vol. 2012, no. 107, pp. 1–8, 2012.

[14] K. Topouzelis, V. Karathanassi, P. Pavlakis, and D. Rokos, "Dark formation detection using neural networks," *Int. J. Remote Sens.*, vol. 29, no. 16, pp. 4705–4720, 2008.

[15] G. Mountrakis, J. Im, and C. Ogole, "Support vector machines in remote sensing: A review," *ISPRS J. Photogramm. Remote Sens.*, vol. 66, no. 3, pp. 247–259, May 2011.

[16] T. Joachims, *Learning to Classify Text Using Support Vector Machines: Methods, Theory and Algorithms*. New York, USA: Springer-Verlag, 2002.

[17] C. N. Long, J. M. Sabburg, J. Calbo, and D. Pages, "Retrieving cloud characteristics from ground-based daytime color all-sky images," *J. Atmos. Ocean. Technol.*, vol. 23, no. 5, pp. 633–652, May. 2006.